This is the accepted manuscript made available via CHORUS. The article has been published as:

Instability of the f-electron state in URu_{2}Si_{2−x}P_{x} probed using high magnetic fields

K. Huang, K.-W. Chen, A. Gallagher, Y. Lai, L. Nelson, D. Graf, and R. E. Baumbach

Phys. Rev. B **99**, 235146 — Published 24 June 2019

DOI: 10.1103/PhysRevB.99.235146

Instability of the f-electron state in $URu_2Si_{2-x}P_x$ probed using high magnetic fields

K. Huang,[1] K. -W. Chen,[1,2] A. Gallagher,[1,2] Y. Lai,[1,2] L. Nelson,[1,2] D. Graf,[1] and R. E. Baumbach[1,2,*]

[1]*National High Magnetic Field Laboratory, Florida State University, Tallahassee, Florida 32306, USA*
[2]*Department of Physics, Florida State University, Tallahassee, Florida 32306, USA*

(Dated: April 23, 2019)

The widely studied Hidden Order phase in URu_2Si_2 exemplifies a broad class of emergent macroscopic states originating from d- and f- electron orbitals and their collective modes. This naturally has resulted in a focus on the associated elements (i.e., U and Ru), but recently it was discovered that electronic tuning on the more passive s- and p-orbitals fundamentally alters the electronic behavior and thus opens opportunities to disentangle the Hidden Order conundrum. Here we present a detailed magnetoresistivity study of $URu_2Si_{2-x}P_x$ which focuses on two important aspects of this topic. First, we show that the anisotropy of the high field ordered states is preserved after Hidden Order is destroyed by Si $\rightarrow$ P chemical substitution, suggesting that this feature is mainly associated with the Kondo lattice; i.e., not Hidden Order itself. Second, Shubnikov-de Haas oscillations reveal that the observable parts of the Fermi surface topography are robust upon approaching the Hidden Order phase boundary and the associated quasiparticle masses remains roughly constant. These observations place constraints on theories and prepare a path towards a resolution to the Hidden Order problem.

Complex collective behavior involving the duality between localized and itinerant electron states has been shown to produce exotic phenomena across a broad spectrum of materials including d-electron high temperature superconductors,[1,2] f-electron superconductors,[3] valence fluctuating systems such as δ-Pu,[4] and others. Amongst these, the intermetallic URu_2Si_2 has continuously attracted interest during the past three decades mainly because it hosts an unknown symmetry breaking ordered state below T_0 = 17.5 K that is referred to as Hidden Order (HO).[5–9] Many theoretical models have been developed for the HO phase and are generally separated by whether the $5f$-electrons are assumed to be more localized or itinerant.[9–19] Significant experimental effort has been invested to test these theories. For instance, ARPES measurements show that the spectral weight is concentrated near the Fermi surface and band structure calculations that include itinerant f-electrons provide the most accurate description of experimental data: i.e., many studies implicate the importance of itinerant electrons.[20–23] However, the angular dependence of the spin zeroes that are observed in the quantum oscillation amplitudes reveal an anistropic g-factor in URu_2Si_2 which is reminiscent of what is seen for localized $5f$-electron moments.[24] Thus, there is an ongoing debate about how to understand the localized/delocalized f-electron duality and its relationship to HO.

Based on this and the multitude of other inconclusive experiments it is clear that alternative routes that expose the fundamentals of HO are still needed. The recent investigation of electron doped $URu_2Si_{2-x}P_x$ series provides an attractive way to do this for several reasons[25,26]: (1) The HO phase is suppressed at very low concentrations ($x_{cr} \approx 0.035$) and for $0.035 < x < 0.26$ the parent compound Kondo lattice is preserved but there is no ordered ground state (NO). Importantly, disorder effects are weak over the NO x-range, as shown by recent ^{29}Si NMR measurements[27]; (2) Si and P are similar in size, which minimizes tuning due to chemical pressure. This is in contrast to what is seen for $URu_{2-x}Fe_xSi_2$, where HO is converted antiferromagnetism in a manner similar to that of applied pressure.[28] (3) Si $\rightarrow$ P substitution only changes the s- and p-electrons and therefore does not directly alter the f or d-electrons, whose importance is laid bare by considering that although there are many chemical variants with the chemical composition MT_2Si_2 (M = lanthanide/actinde and T = transition metal) none of them exhibit HO.[29] Thus, within this series there is the opportunity to disentangle the various factors that might contribute to HO.

In this work we report a detailed investigation of the magnetoresistivity of oriented single crystals of $URu_2Si_{2-x}P_x$. From the angular dependence of the magnetoresistivity, we find that the magnetic field induced phases (previously described in[30]), display a 1/cos(θ) anisotropy is seen as for the parent compound.[31–33] Importantly, this includes x = 0.10 which is in the NO x-region. This shows that the anisotropy is a generic characteristic of the entire series, and thus may not be uniquely associated with HO. We also find that Shubnikov-de Haas quantum oscillations persist up to x = 0.02, which approaches the upper boundary of the HO phase. There is only a small shift in the oscillation frequencies with increasing x, showing that the observable parts of the Fermi surface remain robust even as HO is destabilized. From the temperature dependence of the oscillation amplitudes, we also observe that the quasiparticle effective mass (m_{eff}) remains roughly constant for all x measured for the α- and γ branches. These findings provide useful insights about (i) what distinguishes HO from the underlying Kondo lattice and (ii) what role the Fermi surface plays in setting the conditions for HO, both of which are needed to constrain theory and solve the HO problem.

Single crystals of $URu_2Si_{2-x}P_x$ were grown using a molten indium flux in a resistive tube furnace as reported previously.[25,26] The starting elements had purities of 3N or greater, were combined in a ratio 1(U):2(Ru):2(Si):22(In) and were loaded into sealed 5 cm^3 tantalum crucibles which were then placed in an MTI 1700 °C horizontal tube furnace under flowing argon gas. A zirconium getter was placed in the tube before the tantalum crucible to purify the argon gas at high temperatures. The heating profile was a ramp up to 500 °C at a rate of 50 °C/hour, dwell for 5 hours, ramp up to 600 °C at a rate of 50 °C/hour, dwell for another 5 hours, then ramp up to 1450 °C at a rate of 70 °C/hour. The heat was cycled between

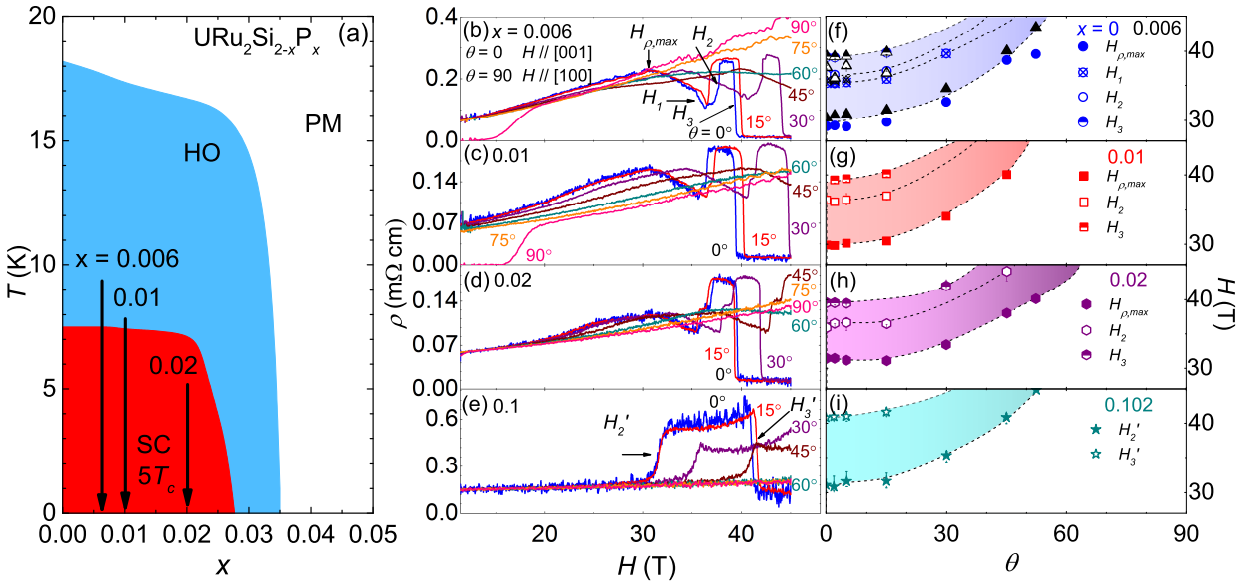

FIG. 1. (Color online)(a) Schematic of the T-x phase diagram.[25,26] The HO and superconducting (SC) phases are represented by the blue and red regions, respectively. The arrows and dashed lines indicate the chemical concentrations measured, shown in the subsequent panels. (b)-(e) The angular dependence of the magnetoresistivity for x = 0.006, 0.01, 0.02, and 0.10, respectively. Representative datasets were chosen with θ increasing by 15° for clarity. θ = 0 corresponds to H//[001] and θ = 90 corresponds to H//[100] with T = 70 mK. The black arrows in (b) represent the critical fields $H_{\rho_{max}}$, H_1, H_2, and H_3 that were observed in concentrations up to x = 0.02. The black arrows in (d) identify H_2' and H_3' for x = 0.10 which is in the NO region. (f)-(i) The right-side panels summarize the critical fields as a function of θ, with panel (f) displaying both x = 0 and 0.006 while (g)-(i) summarizes the results for x = 0.01, 0.02, and 0.10, respectively. The black dashed lines are guides to the eye.

1450 and 1400 °C multiple times and then quenched to room temperature. Excess indium flux was etched by hydrochloric acid. The resulting single crystals were oriented using a Laue x-ray diffractometer to identify the a- [100] and c-axes [001], shown in the supplementary file.[34] The actual chemical composition was determined using electron dispersive spectroscopy measurements.

Multiple features in $\rho(T,\theta)$ are observed, represented by the black arrows in Fig. 1(b), that are consistent with previous studies on the undoped URu_2Si_2 and for Si $\rightarrow$ P substitution.[30–33,35–39] Within the HO x-region we find a series of metamagnetic phase transitions: $H_{\rho_{max}}$ is a peak in $\rho(H)$ that signifies the disruptive effect of the magnetic field on the Kondo lattice; H_1 is a rapid drop in $\rho(H)$ that marks the end of the HO phase; the sudden increase in ρ at H_2 marks the emergence of a spin density wave ordered state; and the rapid decrease in ρ at H_3 corresponds to the onset of the polarized paramagnetic regime. For x = 0.10 (NO), a different resistivity profile is observed.[30] As previously shown, there is a plateau in $\rho(H)$ that begins and ends at H_2' and H_3', respectively. This feature is commensurate with steps in the magnetization and shares a close resemblance to what is observed in 4% Rh substituted specimens (also in the zero field NO regime). In that case the field induced ordered state has a ferrimagnetic up-up-down configuration of the magnetic moments,[40] and we have proposed that a similar type of ordering develops for the Si $\rightarrow$ P substituted materials. Furthermore, for the parent compound the field induced phases are associated with the collapse of the itinerant 5f electron state, and this trend likely persists for substituted specimens.

Summarized in Fig. 1(f)-(i) are the angular dependences of the critical fields. For the undoped URu_2Si_2, all of the observed critical fields ($H_{\rho_{max}}$, H_1, H_2, H_3) display the expected 1/cos(θ) behavior.[31–33] We find that across the HO x-region there is no noticeable change in the anisotropy of the critical fields, and this trend extends into the NO x-region. While it is not yet clear what factors control the anisotropy of the critical fields, we point out that for the parent compound an important feature of the low temperature quasiparticles is that they have an anomalously large Ising anisotropy that is well in excess of the base tetragonal crystalline anisotropy.[21,41–43] For instance, it has been shown that both the superconducting upper critical field and the spin zeroes from quantum oscillation measurements depend on the angular dependence of the g-factor[24,42]: we speculate that the upper field boundaries for the HO phase may be influenced in a similar way. If true, then the Si $\rightarrow$ P substitution series opens an opportunity to establish whether the the large anisotropy is a unique feature of the HO region or is more broadly a feature of the underlying Kondo lattice. In fact, results from Trinh et al.,[41] already suggest that the anisotropy extends well above HO and may be a feature of the underlying strongly correlated electron liquid that is produced by the onset of Kondo coherence. A resolution to this question is essential for developing a theory for the HO state.

More generally, we point out that similar anisotropic behavior has been observed for other Kondo lattice systems including $CeIn_3$ and $CeRhIn_5$.[44,45]

Quantum oscillations are also observed in the magnetoresistivity data (Fig. 1(b)-(d)) for all of the HO samples (up to x = 0.02) with the oscillation amplitude damped for the higher chemically substituted samples due to disorder scattering. To better visualize the oscillations, Fast Fourier transforms (FFT) were performed on the magnetoresistivity data after a smoothed non-oscillating background was subtracted (see Fig. S2).[34] Since the FFT can be affected by the magnetic field fit range, all datasets were analyzed on the range 20 - 45 T, which avoids the metamagnetic phase transitions and superconducting region (further details about variable fit ranges are in the supplementary files).[34] Fig. 2(b)-(e) displays the normalized amplitudes of the FFT profiles for θ = 65° - 120°, with the data offset for clarity. Sharp peaks in the FFT are observed at F = 130 T, 200 T, and 1100 T which correspond to the γ, β, and α branches.[31,46] There is a peak at $F \sim$ 2500 T which can be attributed to a higher harmonic of the α branch, consistent with reported literature.[31,42,46] While the three branches are clear for x = 0 and 0.006, the data become more noisy for x = 0.01 and 0.02, making it difficult to isolate the β and γ branches from the background signal (Fig. 2(c)-(e)). The α peak is clearly observed from θ = 60° - 120° up to x = 0.02, with F_α displaying a maximum around 1200 T near θ = 90°. Upon close examination there appears to be slight shifts to F_α with increasing x, however no discernable trend can be concluded. The branches β and γ display little angular dependence near θ = 90°. A comparison of this with reported literature is illustrated in Fig. 2(a) which summarizes the angular dependence of $F(T)$ and includes the reported values for URu_2Si_2 (red dashed line).[46,47] For α the data matches very well along almost all ranges of θ. For β and γ there are not as much data available for θ = 60° - 120°, yet a simple extrapolation suggests very good agreement with our results.

Electronic band structure calculations show that the α (hole) and γ (electron) branches are centered around the M point while the β (electron) branch corresponds to four semi-spherical pockets located between the Γ and X points.[20,23]. This was confirmed by multiple experimental probes including cyclotron resonance and ARPES.[22,48,49] In the simplest picture, electron doping would raise the Fermi energy and slightly increase the surface area of the β and γ electron pockets while decreasing the surface area for α. From this, the lack of a strong change in the α branch is expected, as the large surface area of the α-branch would require significant changes in the carrier concentration to observe any shift in F_α.[22] Regarding the β branch, there may be a slight increase in F_β with increasing x but we caution that this branch is only observed for x = 0 and 0.006. This insensitivity of the FS to chemical substitution presents a puzzling situation, considering that the HO state abruptly collapses at only slightly larger concentrations ($x_{cr} \approx 0.035$). However, it may be that the case that the FS evolves more strongly in the branches that are not observed. Therefore, further measurements that are not as sensitive to chemical disorder, such as ARPES are of significant interest, especially upon traversing from HO to NO.

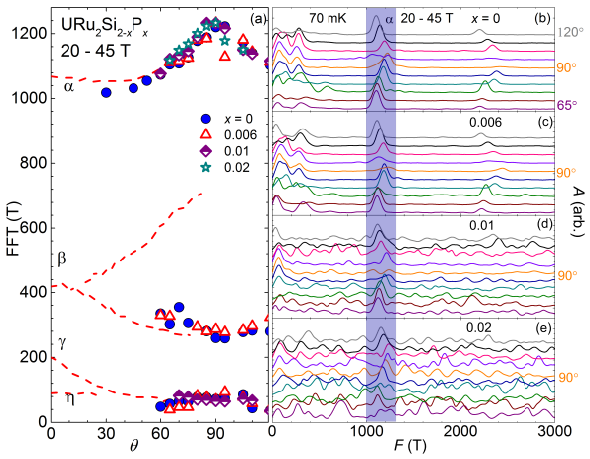

FIG. 2. (Color online)(a) FFT amplitude peak positions vs angle θ are displayed for the α, β, and γ branches in order of decreasing clarity for x up to 0.02. The FFT fit range is 20 - 45 T for all datasets. The α branch displayed the clearest peak, being observable up to x = 0.02 and $\theta > 30°$. Interestingly the observed branches show no significant change with increasing x. The two next observable branches are γ and then β which were seen in x up to 0.01 and 0.006, respectively, and only for $\theta > 60°$. (b)-(e) The right-side panels display the normalized amplitudes of the FFT's for θ = 65° up to 120° for x = 0, 0.006, 0.01, and 0.02, respectively. The data sets are offset for clarity. Highlighted in light blue is the α branch as a guide to the eye.

Displayed in Fig. 3 is $\rho(H)$ at 70 mK for x = 0 - 0.10 for θ = 90° ($H//a$), the angle with the largest amplitude quantum oscillations. Temperature sweeps were performed from T = 70 mK - 780 mK with the FFT displayed in Fig. 3(b)-(e) for x = 0, 0.006, 0.01, and 0.02, respectively. The same FFT range of 20 - 45 T is used for consistency. As expected, increasing temperature damps the quantum oscillations, with α and γ being observable up to T = 780 mK for all x while β could not be determined at 780 mK for x = 0.006. The effective mass, m_{eff}, was determined from Lifshitz-Kosevich fits as displayed in the insets of Panels (b)-(e) In order to establish confidence in the temperature dependence of A and thus the results from the Lifshitz-Kosevich fits, we examined the oscillating part of the magnetoresistivity using different fast fourier transform windows. This is particularly important for the higher x = 0.01 and 0.02, where the amplitudes of the oscillations are significantly dampened. In particular, the FFT was carried out over two field ranges for each data set: (1) H = 20-45 T (shown in the manuscript) and (2) H = 33 - 45 T (shown in the supplementary materials[34]). For x = 0 we find m_{eff} = 6.7, 8.6, and 4.5 for α, β, and γ, respectively, close to reported values of m_{eff} = 7.5, 9, and 3 for α, β, and γ with $H//a$.[46,47] $\rho(H)$ measurements with θ = 76° were also performed and exhibit behavior similar to what is seen at 90°.[34]

The x-dependence of m_{eff} is shown in Fig. 4(a), where it is compared to the evolution of the electronic coefficient of the heat capacity γ_e (Fig. 4(b)) and the Hidden Order temperature (Fig. 4(c)).[25] m_{eff} for the α branch remains roughly constant over most of this x-region, but may exhibit a peak near x =

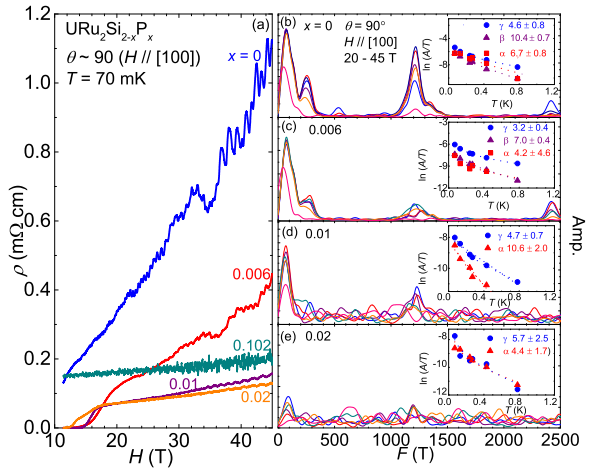

FIG. 3. (Color online)(a) Magnetoresistivity $\rho(H)$ measurements performed in magnetic fields (H) up to 45 T with $H//a$ ($\theta = 90°$). Pronounced oscillations can be observed in all datasets except for $x = 0.10$. (b)-(e) Fast Fourier Transforms (FFT) of $x = 0$, 0.006, 0.01, and 0.02 in (b)-(e), respectively, from $T = 70$ mK up to 780 mK. Amplitude peaks are observed at $F(T) \sim 130$, 200, and 1100 corresponding to the γ, β, and α branches. The insets display the amplitude vs. T. m_{eff} was determined from Lifshitz-Kosevich fits represented by the dashed lines.

0.01. In principle, this trend might suggest the presence of an unknown electronic instability, which was also suggested by bulk measurements including the Sommerfeld coefficient (γ_e), the entropy recovered at T_0, and the size of the jump in the heat capacity at T_c. (Fig. 4(c)).[25] However, as shown in Fig. S5, when the data are analyzed using a different FFT field range the resulting masses differ beyond the error bars, suggesting that this is an artifact of the data analysis procedure. In addition, m_{eff} for the γ branch is constant over this x range. From this, we conclude that both the Fermi surface and m_{eff} are robust up to the point where hidden order abruptly collapses. This is even as the disorder scattering increases, the superconducting upper critical field increases,[25] and the fine structure of the field driven phase transitions is simplified. From this, we infer that the substitution induced changes that are observed within the HO phase are not due to a strong Fermi surface evolution. However, what is still missing is knowledge of (i) the x-dependence of the other Fermi surface branches and (ii) the behavior within the NO region. Therefore it remains important to further investigate this substitution series using probes that track the detailed fermiology (e.g. ARPES), the signatures of broken symmetry (e.g., electronic Raman spectroscopy), and the Kondo lattice hybridization strength (e.g., inelastic neutron scattering, spectroscopic, or tunneling techniques).

To summarize, in this work we performed a detailed magnetoresistivity investigation on the electron-doped $URu_2Si_{2-x}P_x$ system. From angular sweeps of the magnetoresistivity we are able to track several branches of the Fermi surface, especially the α branch. Significantly, many oscillation branches are observable up to $x = 0.02$, which is the highest doped sample still in the HO x-region. We find (i) negligible shifts in the oscillation frequencies and (ii) robust quasiparticle masses with increasing x. Furthermore, the angular dependence of the critical fields reveals a 1 / cos(θ) behavior, even in the NO region. This suggests (i) that the field induced phases that span the entire T-x phase diagram are continuously connected and (ii) that other 1 / cos(θ) anisotropies that have previously been seen in URu_2Si_2 may not be uniquely associated with the HO state.

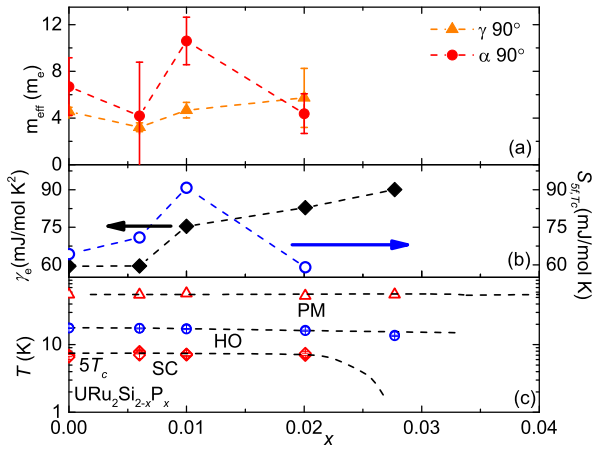

FIG. 4. (Color online) (a) m_{eff} determined from the α and γ branches for $\theta = 90°$ as a function of x. (b) The Sommerfeld coefficient γ_e and entropy from the $5f$ electrons determined from heat capacity measurements. (c) The Kondo, HO, and SC transition temperatures vs. x. The data from (b) and (c) are reproduced from previous literature.[25]

This work was performed at the National High Magnetic Field Laboratory, which is supported by National Science Foundation Cooperative Agreement No. DMR-1157490 and the State of Florida. Research of K. H., Y. L., L. N, D. G., and R. E. B. was supported in part by the Center for Actinide Science and Technology, an Energy Frontier Research Center funded by the US Department of Energy (DOE), Office of Science, Basic Energy Sciences (BES), under Award No. DE-SC0016568. The authors would like to acknowledge Andrés Felipe Santander-Syro for useful discussions. The authors would also like to acknowledge the significant support from the NHMFL DC-field staff, in particular Ju-Hyun Park.

* Corresponding Author: baumbach@magnet.fsu.edu

[1] P. A. Lee, N. Nagaosa, and X.-G. Wen, Rev. Mod. Phys. **78**, 17 (2006).
[2] G. R. Stewart, Rev. Mod. Phys. **83**, 1589 (2011).
[3] C. Pfleiderer, Rev. Mod. Phys. **81**, 1551 (2009).
[4] M. Janoschek, P. Das, B. Chakrabarti, D. L. Abernathy, M. D. Lumsden, J. M. Lawrence, J. D. Thompson, G. H. Lander, J. N. Mitchell, S. Richmond, M. Ramos, F. Trouw, J.-X. Zhu, K. Haule,

G. Kotliar, and E. D. Bauer, Sci. Adv. **1** (2015), 10.1126/sciadv.1500188.
[5] T. T. M. Palstra, A. A. Menovsky, J. van den Berg, A. J. Dirkmaat, P. H. Kes, G. J. Nieuwenhuys, and J. A. Mydosh, Phys. Rev. Lett. **55**, 2727 (1985).
[6] M. B. Maple, J. W. Chen, Y. Dalichaouch, T. Kohara, C. Rossel, M. S. Torikachvili, M. W. McElfresh, and J. D. Thompson, Phys. Rev. Lett. **56**, 185 (1986).
[7] W. Schalbitz, J. Baumann, B. Pollit, U. Rauchschwalbe, H. M. Mayer, U. Ahlheim, and C. D. Bredl, Z. Phys. B. **62**, 171 (1986).
[8] J. A. Mydosh and P. Oppeneer, Rev. Mod. Phys. **83**, 1301 (2011).
[9] J. A. Mydosh and P. M. Oppeneer, Philosophical Magazine **94**, 3642 (2014).
[10] T. Das, Philos. Mag. **94**, 3838 (2014).
[11] Y. Dubi and A. V. Balatsky, Phys. Rev. Lett. **106**, 086401 (2011).
[12] S. Fujimoto, Phys. Rev. Lett. **106**, 196407 (2011).
[13] H. Harmia, K. Miyake, and J. Flouquet, J. Phys. Soc. Japan **79**, 033705 (2010).
[14] C. H. Hsu and S. Chakravarty, Phys. Rev. B **87**, 085114 (2013).
[15] H. Ikeda, M. T. Suzuki, R. Arita, T. Takimoto, T. Shibauchi, and Y. Matsuda, Nature Physics **8**, 528 (2012).
[16] H. Kusunose and H. Harima, J. Phys. Soc. Japan **80**, 084702 (2011).
[17] C. Pepin, M. R. Norman, S. Burdin, and A. Ferraz, Phys. Rev. Lett. **106**, 106601 (2011).
[18] J. G. Rau and H. Y. Kee, Phys. Rev. B **85**, 245112 (2012).
[19] R. Flint, P. Chandra, and P. Coleman, J. Phys. Soc. Japan **83**, 061003 (2014).
[20] J. Q. Meng, P. M. Oppeneer, J. A. Mydosh, P. S. Riseborough, K. Gofryk, J. J. Joyce, E. D. Bauer, Y. Li, and T. Durakiewicz, Phys. Rev. Lett. **111**, 127002 (2013).
[21] A. F. Santander-Syro, M. Klein, F. L. Boariu, A. Nuber, P. Lejay, and F. Reinert, Nature Physics **5**, 637 (2009).
[22] C. Bareille, F. L. Boariu, H. Schwab, P. Lejay, F. Reinert, and A. F. Santander-Syro, Nat. Comms. **7**, 5326 (2014).
[23] P. M. Oppeneer, J. Rusz, S. Elgazzar, M. T. Suzuki, T. Durakiewicz, and J. A. Mydosh, Phys. Rev. B **82**, 205103 (2010).
[24] M. M. Altarawneh, N. Harrison, S. E. Sebastian, L. Balicas, P. H. Tobash, J. D. Thompson, F. Ronning, and E. D. Bauer, Phys. Rev. Lett. **106**, 146403 (2011).
[25] A. Gallagher, K.-W. Chen, C. M. Moir, S. K. Cary, F. Kametani, N. Nikugawa, D. Graf, T. E. Albrecht-Schmitt, S. C. Riggs, A. Shekhter, and R. E. Baumbach, Nat. Comms. **7**, 10712 (2016).
[26] A. Gallagher, K.-W. Chen, S. K. Cary, F. Kametani, D. Graf, T. E. Albrecht-Schmitt, A. Shekhter, and R. E. Baumbach, J. Phys.: Condens. Matter **29**, 024004 (2017).
[27] K. R. Shirer, M. Lawson, T. Kissikov, B. T. Bush, A. Gallagher, K.-W. Chen, R. E. Baumbach, and N. J. Curro, Phys. Rev. B **95**, 041107(R) (2017).
[28] N. Kanchanavatee, M. Janoschek, R. E. Baumbach, J. J. Hamlin, D. A. Zocco, K. Huang, and M. B. Maple, Phys. Rev. B **84**, 245122 (2011).
[29] A. A. Menovsky, A. C. Moleman, G. E. Snel, T. J. Gortenmulder, H. J. Tan, and T. T. M. Palstra, J. of Crystal Growth **79**, 316 (1986).
[30] M. R. Wartenbe, K.-W. Chen, A. Gallagher, N. Harrison, R. D. McDonald, G. S. Boebinger, and R. E. Baumbach, Phys. Rev. B. **96**, 085141 (2017).
[31] D. Aoki, G. Knebel, I. Sheikin, E. Hassinger, L. Malone, T. D. Matsuda, and J. Flouquet, J. Phys. Soc. Japan **81**, 074715 (2012).
[32] Y. J. Jo, L. Balicas, C. Capan, K. Behnia, P. Lejay, J. Flouquet, J. A. Mydosh, and P. Schlottmann, Phys. Rev. Lett. **98**, 166404 (2007).
[33] K. Sugiyama, H. Fuke, K. Indo, K. Shimohata, A. A. Menovsky, J. A. Mydosh, and M. Date, J. Phys. Soc. Japan **59**, 3331 (1990).
[34] K. Huang, K.-W. Chen, A. Gallagher, Y. Lai, L. Nelson, D. Graf, and R. E. Baumbach, Supplementary files.
[35] A. d. Visser, F. R. d. Boer, A. A. Menovsky, and J. J. M. Franse, Solid State Communications **64**, 527 (1987).
[36] M. Jaime, K. H. Kim, G. Jorge, S. McCall, and J. A. Mydosh, Phys. Rev. Lett. **89**, 287201 (2002).
[37] K. H. Kim, N. Harrison, M. Jaime, G. S. Boebinger, and J. A. Mydosh, Phys. Rev. Lett. **91**, 256401 (2003).
[38] G. W. Scheerer, W. Knafo, D. Aoki, G. Ballon, A. Mari, D. Vignolles, and J. Flouquet, Phys. Rev. B **85**, 094402 (2012).
[39] W. Knafo, F. Duc, F. Bourdarot, K. Kuwahara, H. Nojiri, D. Aoki, J. Billette, P. Frings, X. Tonon, E. Lelievre-Berna, J. Floquet, and L. P. Regnault, Nat. Comm. **7**, 1 (2016).
[40] K. Kuwahara, S. Yoshii, H. Nojiri, D. Aoki, W. Knafo, F. Duc, X. Fabrèges, G. W. Scheerer, P. Frings, G. L. J. A. Rikken, F. Bourdarot, L. P. Regnault, and J. Floquet, Phys. Rev. Lett. **110**, 216406 (2013).
[41] J. Trinh, E. Brück, T. Siegrist, R. Flint, P. Chandra, P. Coleman, and A. P. Ramirez, Phys. Rev. Lett. **117**, 157201 (2016).
[42] M. M. Altarawneh, N. Harrison, G. Li, L. Balicas, P. H. Tobash, F. Ronning, and E. D. Bauer, Phys. Rev. Lett. **108**, 066407 (2012).
[43] T. Hattori, H. Sakai, Y. Tokunaga, S. Kambe, T. D. Matsuda, and Y. Haga, Phys. Rev. Lett. **110**, 027001 (2018).
[44] P. J. W. Moll, T. Helm, S.-S. Zhang, C. D. Batista, N. Harrison, R. D. McDonald, L. E. Winter, B. J. Ramshaw, M. K. Chan, F. F. Balakirev, B. Batlogg, E. D. Bauer, and R. F., Nature Quantum Materials **2**, 46 (2017).
[45] F. Ronning, T. Helm, K. R. Shirer, M. D. Bachmann, L. Balicas, M. K. Chan, B. J. Ramshaw, R. D. McDonald, F. F. Balakirev, M. Jaime, E. D. Bauer, and P. J. W. Moll, Nature **548**, 313 (2017).
[46] H. Ohkuni, Y. Inada, Y. Tokiwa, K. Sakurai, R. Settai, T. Honma, Y. Haga, E. Yamamoto, Y. Onuki, H. Yamagami, S. Takahashi, and T. Yanagisawa, Philosophical Magazine B **79**, 1045 (1999).
[47] E. Hassinger, G. Knebel, T. D. Matsuda, D. Aoki, V. Taufour, and J. Flouquet, Phys. Rev. Lett. **105**, 216409 (2010).
[48] S. Tonegawa, K. Hashimoto, K. Ikada, Y.-H. Lin, H. Shishido, Y. Haga, T. D. Matsuda, E. Yamamoto, Y. Onuki, H. Ikeda, Y. Matsuda, and T. Shibauchi, Phys. Rev. Lett. **109**, 036401 (2012).
[49] S. Tonegawa, K. Hashimoto, K. Ikada, Y. Tsuruhara, Y.-H. Lin, H. Shishido, Y. Haga, T. D. Matsuda, E. Yamamoto, Y. Onuki, H. Ikeda, Y. Matsuda, and T. Shibauchi, Phys. Rev. B **88**, 245131 (2013).